World Academy of Science, Engineering and Technology
International Journal of Mechanical and Materials Engineering
Vol:17, No:2, 2023

Fully Automated Methods for the Detection and Segmentation of Mitochondria in Microscopy Images

Blessing Ojeme, Frederick Quinn, Russell Karls, Shannon Quinn

***Abstract*—**The detection and segmentation of mitochondria from fluorescence microscopy is crucial for understanding the complex structure of the nervous system. However, the constant fission and fusion of mitochondria and image distortion in the background make the task of detection and segmentation challenging. Although there exists a number of open-source software tools and artificial intelligence (AI) methods designed for analyzing mitochondrial images, the availability of only a few combined expertise in the medical field and AI required to utilize these tools poses a challenge to its full adoption and use in clinical settings. Motivated by the advantages of automated methods in terms of good performance, minimum detection time, ease of implementation, and cross-platform compactibility, this study proposes a fully automated framework for the detection and segmentation of mitochondria using both image shape information and descriptive statistics. Using the low-cost, open-source Python and OpenCV library, the algorithms are implemented in three stages: pre-processing; image binarization; and coarse-to-fine segmentation. The proposed model is validated using the fluorescence mitochondrial dataset. Ground truth labels generated using Labkit were also used to evaluate the performance of our detection and segmentation model using precision, recall and rand index. The study produces good detection and segmentation results and reports the challenges encountered during the image analysis of mitochondrial morphology from the fluorescence mitochondrial dataset. A discussion on the methods and future perspectives of fully automated frameworks concludes the paper.

***Keywords*—**2D, Binarization, CLAHE, detection, fluorescence microscopy, mitochondria, segmentation.

I. Introduction

MITOCHONDRIA are important intracellular organelles responsible for several metabolic pathways including the production of free energy and the regulation of cellular life and death. Mitochondria fission (division) and fusion (elongation) are two opposing processes whose balance results in the steady-state morphology. Mitochondrial fusion helps to rescue partially damaged mitochondria by exchanging their contents with functional mitochondria while mitochondrial fission enables the removal of damaged mitochondria and facilitates apoptosis during increased levels of cellular stress [1]. Disruption of normal mitochondrial function has been linked to several neurodegenerative diseases relating to aging, including Alzheimer's disease, Huntington's disease, juvenile-onset Parkinson's disease, and cancer. Building a more exact understanding between mitochondrial phenotype and disease is therefore of great significance as the existence of noise and frequent changes in shape among mitochondria (ranging from elongated, fragmented, and tubular-circular and elliptical) makes it challenging to detect subtle differences in morphology and nearly impossible to automate the same [2]. Our open source Organellar Networks (OrNet) framework was designed to perform analyses on diffuse, difficult-to-quantify subcellular structures like mitochondria and actin, but the segmentation procedure still requires some manual input. This process is highly laborious, time consuming, and introduces a varying degree of bias to each labeled image. This leads to improper detection, which in turn, causes a decrease in segmentation accuracy [3]. Thus, it is unable to meet the demands of high-throughput image analysis for which OrNet was designed**.** Additionally, each mitochondrial image typically contains more than one mitochondrion, sometimes touching.

Several methods have been proposed in the literature with different levels of automation to overcome these challenges and quantify the mitochondrial morphology in an unbiased manner. For instance, a number of specialized semi-automatic software tools such as ImageJ [4] IMOD [5], SerialEM [6], CellProfiler [7], and PEET [8] were developed to visually detect and segment volumes of mitochondria to enable accurate interpretation, measurement and detailed analysis. We refer the reader to Eliceiri et al. [9] for an interesting review of various open-source software tools used for the implementation of image data workflow. However, the extremely laborious and time-consuming characteristics of these tools, coupled with the flawed results obtained due to manual annotation processes and their attendant human errors (even with highly trained experts), raised several questions about the practicality of their use in time and safety-critical settings [10]. This drawback birthed inquiries into new research directions for flawless automated mitochondrion detection and segmentation. Inspired by the recent work of Lefebvre et al. [11], the motivation of this study originates from the need to develop a fully automated image analysis tool to detect and segment mitochondrial images directly from the fluorescence microscopy data in a timely, accurate, cross platform compactible manner. Our overarching goal is to utilize information about the shape and sophisticated background knowledge of mitochondrial structure and create a simplified mitochondrial image analysis method for researchers and medical professionals. The algorithms are in three main orderly stages: 1) pre-processing, 2) image binarization, and 3) coarse-to-fine segmentation.

Blessing Ojeme is with the Department of Computer Science, University of Georgia, Athens, GA, USA (corresponding author, phone: 706-540-3525; e-mail: blessing.ojeme@uga.edu).

Frederick Quinn and Russel Karls are with the Department of Infectious Diseases, University of Georgia, Athens, GA, USA.

Shannon Quinn is with the Department of Computer Science, University of Georgia, Athens, GA, USA. He is also with the Department of Cellular Biology, University of Georgia, Athens, GA, USA (e-mail: spq@uga.edu).

The main contributions of the study are as follows:

- *Methods:* We develop a fully automated detection and segmentation model that encodes information for segmentation of 2D mitochondrial morphology from fluorescence microscopy images.
- *Data:* We show that the proposed model enables a single workflow from raw data input to desired detection and 2D segmentation results without relying on pre-trained models or third-party training datasets. It achieves good results in terms of good speed and good performance.

The subsequent sections of this study present the detailed information about related work, methods, implementation, the experimental results and analysis, evaluation, and conclusions.

II. Related Work

The analysis of mitochondria images is essential for studying mitochondrial morphology and computer aided analysis and diagnosis. Segmentation, which is an important step in image processing and diagnostic system, aims to partition an image into a set of meaningful structural parts by assigning labels to pixels so that the pixels with the same label form a segmented object. The output from a segmentation algorithm is an image of the same dimension as the input image where each pixel has been assigned a label indicating which object class the specific pixel belongs to. Generally, mitochondrial image detection and segmentation is a challenging task because of its sophisticated background, continuous cycle of shapes and sizes [10]. The fluorescence microscope, an optical microscope which enables the selective measurement of aggregate size and morphology in cells, has an additional drawback in that its images are corrupted by noise (salt and pepper) and blurred particles from outside of the focal plane, and sub-cellular structures, including synapses and vesicles [4], [12]. Given these challenges, the analysis of mitochondria with automated filtering functionalities and minimal user interference becomes undeniably necessary in order to understand its dynamics and provide much insight on its functioning and role in the well-being of cells [1], [10], [11].

Many brilliant automated methods have been proposed in the literature for its detection [3], [11], [13]-[15] and segmentation [1], [3], [14], [16]-[18]. Ficher et al. [1], for instance, created Mitochondrial Segmentation Network (MitoSegNet), a deep learning segmentation model that enabled researchers to leverage the predictive and analytical strength of deep learning for the analysis of mitochondrial morphology. When tested against three feature-based segmentation algorithms and the machine-learning segmentation tool Ilastik, MitoSegNet outperformed all other methods in both pixelwise and morphological segmentation accuracy. Again, MitoSegNet showed superior performance when applied to unseen fluorescence microscopy images of mitoGFP expressing mitochondria. In an earlier study, Lihavainen et al. [17] developed Mytoe, a software application tool for analyzing mitochondrial morphology and dynamics from fluorescence microscope images. The tool provides automated quantitative analysis of mitochondrial motion by optical flow estimation and of morphology by segmentation of individual branches of the network-like structure of the organelles. Mytoe analyzes a number of features of individual branches, including length, tortuosity and speed, and of the macroscopic structure, such as area of mitochondrial and degree of clustering. Building on the study, Lihavainen et al. [14] developed an automated method for detecting and tracking fluorescent-labeled mitochondria with good accuracy. The MATLAB-based method trained a supervised learning classifier, Random Forest, on small patches extracted from confocal microscope images of U2OS human osteosarcoma cells. In a bid to further improve on the study, Lefebvre et al. [11] developed a fully automated MATLAB-based software package, Mitometer, for analyzing the mitochondrial morphology and fission-fusion dynamics from time-series 2D and 3D fluorescence microscopy TIFF images in a fast and unbiased manner. The experimental results showed that Mitometer was able to accurately measure the morphological features including the sizes and shapes of mitochondria, and dynamic parameters including movement speeds and fission/fusion rates. Building upon an earlier work on active-mask framework developed for the segmentation of confocal fluorescence microscope images, Chen et al. [13] described an automated adaptive region-based distributing function for mitochondrial segmentation from widefield fluorescence microscopy images for quantitative morphology characterization. The model produces good performance against a hand-segmented ground truth and significantly outperforms the original active-mask algorithm, both qualitatively and quantitatively.

A number of traditional machine learning methods, such as support vector machines, k-nearest neighbor algorithm, and adaptive boosting algorithm, have also been described for the tasks of mitochondria detection and segmentation [12], [19]-[21]; for instance, mitochondrial cells were segmented with the Gentle-Boost classifier, trained with histograms of gray scale and Gabor-based filter responses computed in neighborhood windows on each pixel [3].

III. The Proposed Model

Evidently, most of the studies on automated bio-image processing in the literature focus primarily on matrix laboratory (MATLAB), machine learning, and deep learning-based analytics [19], with simple automated methods from raw data currently receiving little attention. While these approaches and platforms are very powerful and present excellent image processing workstations for various data analytical projects, a number of significant challenges which limit their use have also been identified. For instance, the comparatively high costs of MATLAB in terms of fast computers with sufficient memory requirements, and the cost of obtaining the licensed version make it undesirable for a large number of programming students and research communities [22]. Additionally, the slow execution of programs created in the MATLAB environment puts a limit to its use in the development of real-time or time-critical image processing applications [22].

The full potential of machine learning and deep learning algorithms is dependent on the availability of a sufficient amount of ground-truth labeled data [23]. While this is helpful

in ensuring efficiency, it also exposes it to certain limitations and potential limited efficiency [24]. Generating ground-truth labeled data for machine learning and deep learning methods is a tedious process and does not guarantee a perfect segmentation result. Again, deep learning methods are associated with some significant challenges, which limit their use in segmentation tasks. These include 1) significantly slow speed due to maxpool operation, 2) high computational cost [23], and 3) longer training process due to multiple layers [25], [26]. Given these drawbacks, this study investigates other practical methods for solving medical image segmentation problems with high reliability, low cost and accuracy.

We propose a fully automated model that yields good segmentation results from raw data input without relying on pre-trained models or third-party training datasets. Our model is developed in open-source Python and the OpenCV library, which offer easy ways to manipulate color spaces while remaining fast and easy to use on any laptop or workstation [27]. Additionally, the OpenCV and Python development environments give our tool the added advantage of not being limited to particular file formats [22], data modalities, and can be quickly adapted to new experimental designs [28]. Our system can also be installed on a small low-memory computer with low electrical power usage, making it much more suitable as an efficient resource for mitochondrial image processing systems [27].

IV. Methods

As shown in Fig. 1, we introduce a fully automated method for the detection and segmentation of mitochondria using the three methodological steps described in this section. The algorithms have been implemented in python in our OrNet framework for fluorescence microscopy image processing and are available upon request.

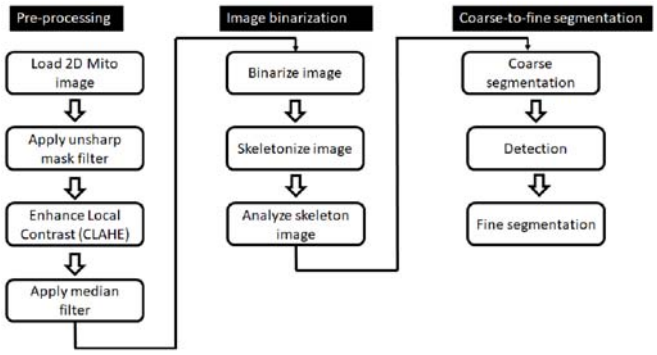

Fig. 1 Methodological steps of the study

1) Image pre-processing: The image pre-processing helps to improve the image quality and ensures the high accuracy of the binarization stage. After loading the mitochondrial image, pre-processing was performed in the following three stages:

i. filter application for unsharp masking: this was done to improve the sharpness of the edges and interfaces of images that contain depth information. Mathematically, this is defined as:

$$m(x,y) = f(x,y) - f_b(x,y) \quad (1)$$

where $f(x,y)$ represents the original image and $f_b(x,y)$ represents the blurred version of the original image. Then this mask is added back to the original image, which results in enhancing the high-frequency components $g(x,y) = f(x,y) + k * m(x,y)$ where k represents the portion of the mask to be added. Unsharp masking occurs when $k = 1$, but high boost filtering occurs when $k > 1$. The opencv library achieves the unsharp masking using the functions: *cv2.GaussianBlur* and *cv2.addWeighted.*

ii. Next, we apply the Contrast Limited Adaptive Histogram Equalization (CLAHE) filter to help improve the contrast of the images, as described in [29]. CLAHE function is included in the OpenCV package in two parameters: *clipLimit* (representing the threshold clip size) and *tileGridSize* (representing the size of the image processing window). *(cv2.createCLAHE(clipLimit=2.0,tileGridSize=(gridsize,gridsize))*.

iii. Finally, we experimented with mean, median, bilateral and blur filters to help reduce the amount of noise present in the images. The results show the median filter outperforming the other filters in terms of noise reduction and edge preservation. This was followed by the mean filter, which blurs edges as it averages real signal with the background. The median filter is applied to a specified radius of two pixels. Median filtering functionality is implemented in the OpenCV packages using *cv2.medianBlur()* function. In summary, the unsharp masking and CLAHE help to amplify the salt and pepper noise of the fluorescent images, while the median filter helps to reduce or eliminate this type of noise [29].

2) Image binarization: On completion of the image pre-processing stage, we binarized the image by applying a threshold on the intensity of all pixels in the image. This was a necessary step to separate the background and other non-mitochondrial tissues and to make the task of segmentation and identification of the mitochondrial images less difficult and challenging [3]. This was achieved in the following two stages:

1) We binarized the mitochondrial images using the intensity-based thresholding to help create a mask on the mitochondria and separate the regions of interest in the mitochondria image from regions that do not contain relevant information (background). The intensity-based thresholding T is available as cv2.threshold() on the OpenCV library. The image will be a binary image according to:

$$g(x,y) = \begin{cases} 1, & if\ f(x,y) > T \\ 0, & if\ f(x,y) \le T \end{cases} \quad (2)$$

To ensure the stability of the mask, we run a parameter exploration algorithm to select the standard deviation of the kernel and the threshold level.

2) We skeletonized the image by removing small regions, and then compute the descriptive statistics describing the skeleton. Skeletonized image represents the image topology and is useful for feature extraction. OpenCV provides for skeletonization process by morphology using the *cv2.erode()* (erosion), *cv2.dilate()* (dilation) and *cv2.subtract()* (subtraction) functions. Since the input coarse segmented regions of this stage are quite isolated and small, various kinds of segmentation methods were adopted for this stage. We applied similar gradient boundary enhancement and combination of image binarization operations used during the coarse segmentation stage, to improve the segmentation task and arrive at the finely segmented mitochondrial regions.
3) Coarse-to-fine segmentation: The mitochondrial image data have a sophisticated background, with mitochondria in close proximity to vesicles or various membranes. This violates the standard assumption that strong image gradient always corresponds to significant boundaries and makes many state-of-the-art segmentation and classification algorithms, powerless [10]. In order to address this challenge, this study improves upon the earlier approaches in the following two aspects:

i. We adopted the coarse and fine segmentation procedure described in [3] and [10]. The coarse segmentation, achieved in the image binarization stage (Fig. 1 (f)) helped us to identify and include regions of high concentration of mitochondria based on its circular and elliptical shapes, and exclude regions of non-mitochondria or low concentration of mitochondria.

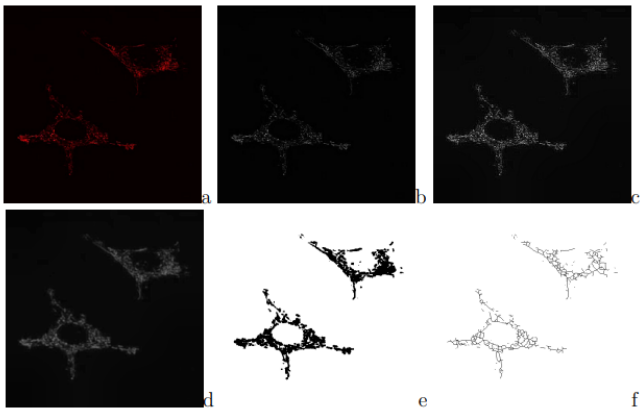

Fig. 2 (a) Original image (b) Unsharp image (c) CLAHE image (d) Median (e) Binary (f) Skeleton

Having performed the coarse segmentation, we performed the fine segmentation stage to improve the segmentation of mitochondria by removing non-mitochondrial pixels, which touch in coarse mitochondrial regions. We applied a combination of gradient boundary enhancement used to achieve the coarse segmentation for small regions of mitochondria. Examples for each of coarse and fine segmentation results are illustrated in Fig. 3. It can be seen that the fine segmentation results are largely improved compared to coarse segmented versions of the original mitochondrial image.

ii. The study experimented with several images in the listeriolysin O (llo), mitochondrial division inhibitor (mdivi) and control datasets using several pre-processing and binarization algorithms that have achieved promising results (in terms of fast speed, good performance, and having been implemented in the OpenCV framework) in medical image identification, segmentation, and classification.

The process of mitochondrial segmentation was split into two: coarse and fine segmentation using the shape information and descriptive statistics. For the coarse segmentation, we adopted the method used in [3] in order to enhance the mitochondrial boundaries that may not be clear. OpenCV provides for gradient enhancement in three functions: *cv2.Sobel()* (Sobel), *cv2.scharr()* (Scharr), and *cv2.Laplacian()* (Laplacian). Having achieved good performance in many image segmentation applications [30], this study applied the Sobel gradient enhancement. It uses two kernels measuring pixels to calculate the gradient.

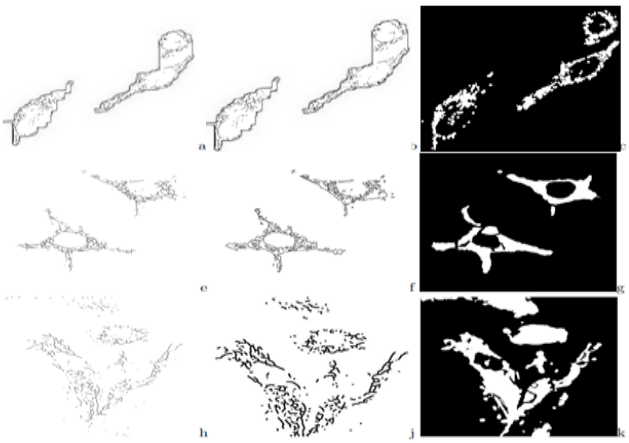

Fig. 3 Coarse, fine segmentation and ground truth labels of mitochondria from three datasets (llo, mdivi and control): a = coarse segmentation for llo; b = fine segmentation for llo; c = ground truth for llo; d = coarse segmentation for mdivi; f = fine segmentation for mdivi; g = ground truth for mdivi; h = coarse segmentation for control; j = fine segmentation for control; ground truth for control

V. Experimental Results and Analysis

The analytical framework comprised detection and segmentation of mitochondrial from raw dataset, which is a collection of confocal imaging videos of live HeLa cells fluorescently tagged with the protein DsRed2-Mito-7 [31]. It comprises three distinct groups of cells: the listeriolysin O (llo) group that was exposed to a pore-forming toxin, to induce mitochondrial fragmentation; the mitochondrial division inhibitor 1 (mdivi) group that was exposed to mitochondrial division inhibitor 1 (mdivi) to induce mitochondrial fusion, and the control group that was not exposed to any external stimulant. Every imaging video consists of at least 20,000 frames, of dimensions 512 x 512, captured at 100 frames per second. Fig. 3 represents each of coarse and fine segmentation

of the llo, mdivi and control datasets.

In this paper, we present a fully automated method for mitochondria detection and segmentation in fluorescence microscopy images. The proposed framework is able to automatically detect mitochondria in a 2D context without any user interaction. The algorithm was tested on several images from llo, mdivi and control datasets.

From the binarized image, we computed the area occupied by mitochondrial structures before the image was skeletonized. The descriptive parameters, mean and standard deviation were computed from the skeletonized image. Table I shows the computed values of the coarse and fine segmentation for the llo, mdivi, and control dataset. The area denotes the total area occupied by mitochondria (footprint) after being separated from the background. The results demonstrate that all images segmented in the three datasets (llo, mdivi and control) exhibited a statistically equal area (denoting mitochondrial images occupying almost an equal area) when compared with the ground truth. This agrees with the definition of segmentation that the output from a segmentation algorithm is an image of the same dimension as the input image where each pixel has been assigned a label indicating which object class the specific pixel belongs to.

TABLE I
MEASUREMENT OF COARSE AND FINE SEGMENTATION AND GROUND TRUTH

	Area	Mean	Standard Deviation
Coarse segmentation for llo	262144	249.317	30.275
Fine segmentation for llo	262144	228.825	66.717
Ground truth for llo	262144	34.496	87.215
Coarse segmentation for mdivi	262144	3.041	27.68
Fine segmentation for mdivi	6185	255	0
Ground truth for mdivi	262144	22.121	71.775
Coarse segmentation for control	262144	3.017	27.574
Fine segmentation for control	247711	0	0
Ground truth for control	262144	51.288	102.216

VI. EVALUATION

In order to quantitatively evaluate the performance of the model, we generated several ground truth labels from each of the three datasets using Labkit. [24]. Labkit is a user-friendly Fiji plugin platform that provides automated and manual image segmentation routines, which can be quickly applied to single and multi-channel 2D or 3D images as well as to time-lapse movies. Our choice of Labkit was motivated by the remarkable results it achieved in a number of recent studies where it was used for ground truth generation [10], [13], [26]. We paired each frame containing the mitochondria detected and segmented by our method with the corresponding ground truth frame and computed the descriptive statistics (mean and standard deviation). The results of all measurements are shown in Table I. We also evaluated the proposed model using three commonly used metrics: precision, recall, and rand index. Precision, also known as the positive predictive value, measures the proportion of positively detected labels that are actually correct. A model that achieves high precision has minimal false negatives. Mathematically, precision is given as:

$$Precision = \mathrm{TP}/(\mathrm{FP} + \mathrm{TP})$$

Recall, also called sensitivity or true positive rate (TPR), measures the model's ability to correctly detect the positives out of actual positives. That is, it measures how good the model is at identifying all actual positives out of all the positives that exist within the image data. A model that achieves high recall has minimal false positives. Mathematically, the recall is given as:

$$Recall = \mathrm{TP}/(\mathrm{FN} + \mathrm{TP})$$

where TP = true positive, FP = false positive, and FN = false negative.

The Rand Index (RI) between test and ground-truth segmentations S and G is given by the sum of the number of pairs of pixels that have the same label in S and G and those that have different labels in both segmentations, divided by the total number of pairs of pixels. RI is given as:

$$RI = (a + b)/(a + b + c + d)$$

where, a represents number of pairs of elements in S that are in the same set in U and in the same set in V; b represents the number of pairs of elements in S that are in different sets in U and in different sets in V; c represents the number of pairs of elements in S that are in the same set in U and in different sets in V; d represents the number of pairs of elements in S that are in different sets in U and in the same set in V. The range of RI values is between 0 and 1, where 0 is for absolute non-compliance with GT and 1 is for total compliance with GT.

TABLE II
EVALUATION METRICS

	Precision	Recall	Rand index
Coarse segmentation for llo	0.88	0.82	0.84
Fine segmentation for llo	0.92	0.91	0.84
Ground truth for llo	1.00	1.00	1.00
Coarse segmentation for mdivi	0.72	0.86	0.79
Fine segmentation for mdivi	0.89	0.87	0.87
Ground truth for mdivi	1.00	1.00	1.00
Coarse segmentation for control	0.86	0.84	0.90
Fine segmentation for control	0.93	0.81	0.77
Ground truth for control	1.00	1.00	1.00

VII. CONCLUSIONS AND FUTURE WORK

The three-stage framework described in this paper provides automated computer-assisted tools to address a variety of challenges often faced during the detection and segmentation of mitochondrial imagery in video. It relies on: I) the pre-processing stage to decrease the amount of noise, amend the effects of the missing edge, and prepare the image for subsequent steps; II) the image binarization stage to help separate the mitochondrial regions from the non-mitochondrial regions; and, III) the coarse-to-fine segmentation stage to accomplish the detection and segmentation methods. Even though the proposed method in this study illustrated a simple and good performance implementation, there were a number of

challenges encountered during the study. These include the detection process and information fusion process that need to be addressed. These challenges stem from the fact that some mitochondria may not have been detected especially if they display extremely elongated shapes or do not present the mitochondrial structure characteristics. An interesting future research direction would be to explore the use of other fully automated detection and segmentation algorithms, such as machine learning and deep learning methods, and then do a comparison between the two methods, a coarse-to-fine method and a direct segmentation method. Future research in this area will investigate the two methods, and will focus on optimizing the segmentation results.

Declaration of Competing Interests

We declare that we have no known competing financial interests or personal relationships that could have appeared to influence the work reported in this paper.

Acknowledgment

This work was supported by award 1R21AI151453-01A1 from the National Institutes of Health (NIH).

References

[1] C. A. Fischer *et al.*, "MitoSegNet: Easy-to-use Deep Learning Segmentation for Analyzing Mitochondrial Morphology," *iScience*, vol. 23, no. 10, Oct. 2020, doi: 10.1016/j.isci.2020.101601.

[2] F. Troger *et al.*, "Identification of mitochondrial toxicants by combined in silico and in vitro studies – A structure-based view on the adverse outcome pathway," *Comput. Toxicol.*, vol. 14, May 2020, doi: 10.1016/j.comtox.2020.100123.

[3] N. Nguyen-Thanh, T. Pham, K. Ichikawa, and T. D. Pham, "Automated Detection and Segmentation of Mitochondrial Images based on Gradient Enhancement and Adaptive Gabor Filter," 2019. (Online). Available: https://hal.archives-ouvertes.fr/hal-02284786

[4] A. J. Valente, L. A. Maddalena, E. L. Robb, F. Moradi, and J. A. Stuart, "A simple ImageJ macro tool for analyzing mitochondrial network morphology in mammalian cell culture," *Acta Histochem.*, vol. 119, no. 3, pp. 315–326, Apr. 2017, doi: 10.1016/j.acthis.2017.03.001.

[5] S. Xu, O. Amira, J. Liu, C. X. Zhang, J. Zhang, and G. Li, "HAM-MFN: Hyperspectral and multispectral image multiscale fusion network with RAP loss," *IEEE Trans. Geosci. Remote Sens.*, vol. 58, no. 7, pp. 4618–4628, Jul. 2020, doi: 10.1109/TGRS.2020.2964777.

[6] E. O'Toole, P. van der Heide, J. Richard McIntosh, and D. Mastronarde, "Large-Scale Electron Tomography of Cells Using SerialEM and IMOD," *Hanssen, E. Cell. Imaging. Biol. Med. Physics, Biomed. Eng. Springer, Cham. https//doi.org/10.1007/978-3-319-68997-5_4*, pp. 95–116, 2018, doi: 10.1007/978-3-319-68997-5_4.

[7] C. McQuin *et al.*, "CellProfiler 3.0: Next-generation image processing for biology," *PLoS Biol.*, pp. 1–17, 2018.

[8] L. Henderson and M. Beeby, "High-Throughput Electron Cryo-tomography of Protein Complexes and Their Assembly," *Marsh, J. Protein Complex Assem. Methods Mol. Biol. vol 1764. Humana Press. New York, NY. https//doi.org/10.1007/978-1-4939-7759-8_2*, vol. 01, pp. 29–44, 2018.

[9] K. W. Eliceiri *et al.*, "Biological Imaging Software Tools," *Nat Methods*, vol. 9, no. 7, pp. 697–710, 2013, doi: 10.1038/nmeth.2084.Biological.

[10] W. Li, H. Deng, Q. Rao, Q. Xie, X. Chen, and H. Han, "An automated pipeline for mitochondrial segmentation on ATUM-SEM stacks," in *Journal of Bioinformatics and Computational Biology*, Jun. 2017, vol. 15, no. 3. doi: 10.1142/S0219720017500159.

[11] A. E. Y. T. Lefebvre, D. Ma, K. Kessenbrock, D. A. Lawson, and M. A. Digman, "Automated segmentation and tracking of mitochondria in live-cell time-lapse images," *Nat. Methods*, vol. 18, no. 9, pp. 1091–1102, Sep. 2021, doi: 10.1038/s41592-021-01234-z.

[12] C. H. Chu, W. W. Tseng, C. M. Hsu, and A. C. Wei, "Image Analysis of the Mitochondrial Network Morphology with Applications in Cancer Research," *Frontiers in Physics*, vol. 10. Frontiers Media S.A., Apr. 13, 2022. doi: 10.3389/fphy.2022.855775.

[13] K. C. J. Chen, Y. Yu, R. Li, H. C. Lee, G. Yang, and J. Kovačevič, "Adaptive active-mask image segmentation for quantitative characterization of mitochondrial morphology," in *Proceedings - International Conference on Image Processing, ICIP*, 2012, pp. 2033–2036. doi: 10.1109/ICIP.2012.6467289.

[14] E. Lihavainen, J. Mäkelä, J. N. Spelbrink, and A. S. Ribeiro, "Detecting and Tracking the Tips of Fluorescently Labeled Mitochondria in U2OS Cells", doi: 10.1007/978-3-319-23234-8.

[15] E. U. Mumcuoglu, R. Hassanpour, S. F. Tasel, G. Perkins, M. E. Martone, and M. N. Gurcan, "Computerized detection and segmentation of mitochondria on electron microscope images," *J. Microsc.*, vol. 246, no. 3, pp. 248–265, Jun. 2012, doi: 10.1111/j.1365-2818.2012.03614.x.

[16] R. J. Giuly, M. E. Martone, and M. H. Ellisman, "Method: Automatic segmentation of mitochondria utilizing patch classification, contour pair classification, and automatically seeded level sets," *BMC Bioinformatics*, vol. 13, no. 1, Feb. 2012, doi: 10.1186/1471-2105-13-29.

[17] E. Lihavainen, J. Mäkelä, J. N. Spelbrink, and A. S. Ribeiro, "Mytoe: Automatic analysis of mitochondrial dynamics," *Bioinformatics*, vol. 28, no. 7, pp. 1050–1051, Apr. 2012, doi: 10.1093/bioinformatics/bts073.

[18] S. F. Tasel, R. Hassanpour, E. U. Mumcuoglu, G. C. Perkins, and M. Martone, "Automatic detection of mitochondria from electron microscope tomography images: a curve fitting approach," in *Medical Imaging 2014: Image Processing*, Mar. 2014, vol. 9034, p. 903449. doi: 10.1117/12.2043517.

[19] G. M. Fogo *et al.*, "Machine learning-based classification of mitochondrial morphology in primary neurons and brain," *Sci. Rep.*, vol. 11, no. 1, Dec. 2021, doi: 10.1038/s41598-021-84528-8.

[20] R. Narasimha, H. Ouyang, A. Gray, S. W. McLaughlin, and S. Subramaniam, "Automatic joint classification and segmentation of whole cell 3D images," *Pattern Recognit.*, vol. 42, no. 6, pp. 1067–1079, Jun. 2009, doi: 10.1016/j.patcog.2008.08.009.

[21] A. Zahedi *et al.*, "Deep Analysis of Mitochondria and Cell Health Using Machine Learning," *Sci. Rep.*, vol. 8, no. 1, Dec. 2018, doi: 10.1038/s41598-018-34455-y.

[22] C. Ozgur, T. Colliau, G. Rogers, and Z. Hughes, "MatLab vs. Python vs. R," *J. Data Sci.*, vol. 15, no. 3, pp. 355–372, 2021, doi: 10.6339/jds.201707_15(3).0001.

[23] M. H. Hesamian, W. Jia, X. He, and P. Kennedy, "Deep Learning Techniques for Medical Image Segmentation: Achievements and Challenges," *J. Digit. Imaging*, vol. 32, no. 4, pp. 582–596, 2019, doi: 10.1007/s10278-019-00227-x.

[24] M. Arzt *et al.*, "LABKIT: Labeling and Segmentation Toolkit for Big Image Data," *Front. Comput. Sci.*, vol. 4, no. February, pp. 1–12, 2022, doi: 10.3389/fcomp.2022.777728.

[25] F. Altaf, S. Islam, N. Akhtar, and N. Janjua, "Going deep in medical image analysis: Concepts, methods, challenges, and future directions," *IEEE Access*, vol. 7, pp. 99540–99572, 2019, doi: 10.1109/ACCESS.2019.2929365.

[26] G. Varoquaux and V. Cheplygina, "Machine learning for medical imaging: methodological failures and recommendations for the future," *npj Digit. Med.*, vol. 5, no. 1, 2022, doi: 10.1038/s41746-022-00592-y.

[27] C. E. Widodo, K. Adi, and R. Gernowo, "Medical image processing using python and open cv," *J. Phys. Conf. Ser.*, vol. 1524, no. 1, pp. 8–12, 2020, doi: 10.1088/1742-6596/1524/1/012003.

[28] D. Yatsenko *et al.*, "DataJoint: managing big scientific data using MATLAB or Python," *bioRxiv*, pp. 1–10, 2015.

[29] G. Yadav, S. Maheshwari, and A. Agarwal, "Contrast limited adaptive histogram equalization based enhancement for real time video system," *Proc. 2014 Int. Conf. Adv. Comput. Commun. Informatics, ICACCI 2014*, pp. 2392–2397, 2014, doi: 10.1109/ICACCI.2014.6968381.

[30] A. Asmaidi, D. S. Putra, M. M. Risky, and F. U. R, "Implementation of Sobel Method Based Edge Detection for Flower Image Segmentation," *SinkrOn*, vol. 3, no. 2, p. 161, 2019, doi: 10.33395/sinkron.v3i2.10050.

[31] M. Hill *et al.*, "Spectral Analysis of Mitochondrial Dynamics: A Graph-Theoretic Approach to Understanding Subcellular Pathology," *Proc. 19th Python Sci. Conf.*, no. Scipy, pp. 91–97, 2020, doi: 10.25080/majora-342d178e-00d.